Available online at www.sciencedirect.com
ScienceDirect
Journal of Power Sources 166 (2007) 239–243
JOURNAL OF POWER SOURCES
www.elsevier.com/locate/jpowsour

Short communication

Particle size dependence of the lithium storage capability and high rate performance of nanocrystalline anatase TiO_2 electrode

Chunhai Jiang [a], Mingdeng Wei [b], Zhimei Qi [b], Tetsuichi Kudo [a], Itaru Honma [a], Haoshen Zhou [a,b,*]

[a] *Energy Technology Research Institute, National Institute of Advanced Industrial Science and Technology (AIST), Umezono 1-1-1, Tsukuba, Ibaraki 305-8568, Japan*
[b] *Japan Science and Technology Agency (JST), PRESTO, Kawagoe, Saitama 332-0012, Japan*

Received 4 September 2006; received in revised form 28 December 2006; accepted 4 January 2007
Available online 14 January 2007

Abstract

The lithium storage capability and high rate performance of nanocrystalline anatase TiO_2 electrodes are highly dependent on the particle sizes. The electrode made from a very fine anatase powder of 6 nm exhibited the highest capacity even at high current rates. It is believed that increasing the specific surface area of the nanocrystalline anatase electrodes has increased the weight ratio of the atoms resided near or on the surface layers and hence improved the surface Li storage; whereas decreasing the particle size has reduced the transport length for Li insertion in the bulk of anatase phase, and so made the Li insertion more efficiently. Besides that, it is found that the specific capacity contributed by the surface Li storage was very stable upon cycling or increasing the current rate; whereas the short Li diffusion length could greatly facilitate the Li insertion/extraction in/from the bulk of the anatase electrode. These two features of nanocrystalline anatase electrodes resulted in very good cycle performance.

Keywords: Nanocrystalline anatase TiO_2; Lithium insertion; High rate performance

1. Introduction

Anatase TiO_2 is an interesting electrode material in rechargeable lithium ion batteries, not only because it may reversibly uptake 0.5 Li in per formula unit of TiO_2, but also because it is a fast Li insertion/extraction host [1–5]. Utilizing these two features of anatase TiO_2 electrodes, lithium ion batteries with high power and high energy densities can be anticipated.

The intercalation mechanism of Li ions into anatase has been studied in a variety of experimental and theoretical works [6–10]. The Li insertion/extraction in/from anatase TiO_2 can be described by the following equation:

$$TiO_2 + xLi^+ + xe^- \leftrightarrow Li_xTiO_2$$

Upon Li insertion, the anatase converts to a two-phase product, including the Li-poor $Li_{0.05}TiO_2$ (space group $I4_1/amd$) and the Li-rich $Li_{0.5}TiO_2$ (space group *Imma*) phases [11]. The insertion of positively charged Li ions has to be balanced with an uptake of electrons to keep the overall charge neutrality. The Li ions are randomly distributed over half of the available interstitial octahedral sites, leading to a theoretical capacity of 167.5 mAh g^{-1} [12].

For practical devices the extent, reversibility and speed of Li insertion/extraction are of extremely important. An effective way to meet these demands is to develop nanostructured electrodes [13]. In recent years, nanostructured anatase electrodes are being actively investigated [13–18], basically because of their shorter length for both electronic and Li^+ transport, higher electrode–electrolyte contact area, and better accommodation of the strain of Li insertion/extraction. Besides that, due to the very high specific surface area, the lithium reaction mechanism in nanocrystalline anatase electrodes is somewhat unusual in comparison to that of micrometer-sized electrodes, but not well understood, such that they show an extra Li accommodation [15]. Up to now, a systematic study of the particle size effect

* Corresponding author at: Energy Technology Research Institute, National Institute of Advanced Industrial Science and Technology (AIST), Umezono 1-1-1, Tsukuba, Ibaraki 305-8568, Japan. Tel.: +81 29 861 5795; fax: +81 29 861 5799.
E-mail address: hs.zhou@aist.go.jp (H. Zhou).

0378-7753/$ – see front matter © 2007 Elsevier B.V. All rights reserved.
doi:10.1016/j.jpowsour.2007.01.004

on the Li storage capability, especially the high rate performance, in anatase electrode was still lack. With this concern, we will present the results of such a systematic investigation in this paper. Especially, the contribution of the short Li diffusion length and the high specific surface area of nanocrystalline anatase electrodes to the high capacity and high rate performance were separately discussed, which may clearly reveal the advantages of the nanostructured electrodes over the micrometer-sized ones as the Li insertion hosts.

2. Experimental

Commercially available anatase nano-powders with particle (crystallite) size of 6 (hereafter denoted as A6), 15 (A15), and 30 nm (A30) (Tayca Corp., Japan) were used as obtained. The detailed data of these powders, such as the crystallite size and specific surface area, were listed in Table 1. To prepare the electrodes, the anatase powders were mixed with acetylene black carbon (AB) and teflon (poly(tetrafluoroethylene)) in a weight ratio of 50:45:5 and ground thoroughly. The mixtures were then pressed onto nickel mesh (100 mesh) as the working electrode. Li metal pressed on the nickle mesh was used as the reference and counter electrodes. Galvanostatic discharge–charge measurements were performed in 1 M $LiClO_4$ in EC + DMC (EC/DMC = 1/1, v/v) between voltage limits of 1.0–3.5 V (Li^+/Li) under constant current densities of 0.1, 1, 10 and 40 A g^{-1}. The weight in specific capacity and current density was calculated based on the active material (TiO_2) only.

3. Results and discussion

Fig. 1 depicts the second discharge and charge curves of the anatase electrodes with different particle sizes cycled at 0.1 A g^{-1} (~0.6 C, 1 C = 167.5 mA g^{-1}). The Li storage capability of anatase electrode is strongly dependent on the particle size, namely, the smaller the particle size, the higher the capacity. For example, the specific discharge capacity of A6 is 234 mAh g^{-1}, corresponding to $x = 0.7$ in Li_xTiO_2; whereas these values are 210 and 203 mAh g^{-1} for A15 and A30, respectively. Clearly, using ultrafine anatase electrode can effectively improve the Li storage capability. In a very recent work, Subramanian et al. [18] also reported that a nanocrystalline anatase powder of 10 nm showed a second discharge capacity of 180 mAh g^{-1} at a constant current density of 0.13 mA cm^{-2}. And also, the capacity decreased with increasing the particle sizes. In our experiments, 0.1 A g^{-1} approximately corresponds to 0.4 mA cm^{-2}. Even the higher mass ratio of carbon black used in our study may decrease somewhat the real current density, the capacity data presented here is still higher than that reported in ref. [18].

Table 1
Detailed information of the used commercial anatase nano-powders

Sample name	Product name	Lot no.	Particle (crystallite) size (nm)	Specific surface area (m^2 g^{-1})
A6	AMT-100	0134J	6	258
A15	TKP-102	1204	15	83
A30	AMT-600	6530J	30	57

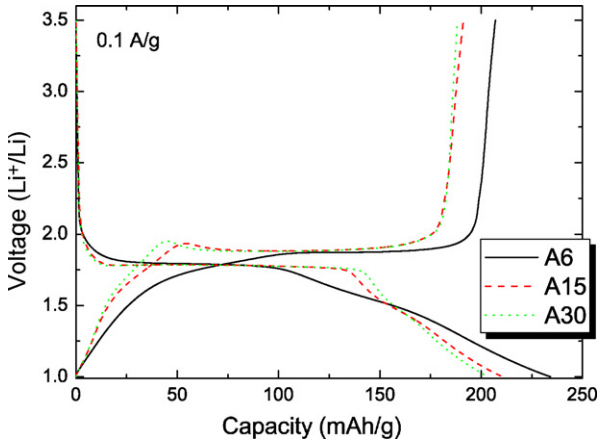

Fig. 1. The second discharge–charge profiles of the nanocrystalline anatase electrodes with different particle sizes cycled at 0.1 A g^{-1}.

Seeing more closely to Fig. 1, we may find that the Li insertion/extraction processes in anatase were also influenced by particle sizes. For example, the Li insertion plateau (at ca. 1.78 V (Li^+/Li)) of A6 is shorter than those of A15 and A30. A large part of the high discharge capacity of A6 is due to the long sloped-region from 1.78 to 1.0 V (Li^+/Li). This plateau indicates the phase equilibrium between anatase TiO_2 and anatase $Li_{0.5}TiO_2$, within which half of Ti^{4+} is converted to Ti^{3+} along with the insertion of Li ions. The length of this biphasic region corresponds to the number of lithium ions inserted into the crystal lattice of anatase (hereafter we call it bulk anatase) based on the Faradaic mechanism. The shorter biphasic region of A6 suggests that although it has the smallest particle size, i.e., the shortest Li diffusion length for the easiest Li insertion, the Li ions inserted into the bulk anatase are less than that in A15 and A30. In other words, the available interstitial octahedral sites for Li insertion have been reduced by decreasing the crystallite size of the anatase electrode.

The short biphasic region of A6 is thought to be related to its very high specific surface area (258 m^2 g^{-1}). Li ions can be inserted into both the surface and bulk of the nanostructured anatase electrode, but based on different mechanisms [10]. For a given amount of anatase powders, increasing the specific surface area will inevitably increase the proportion of the total number of atoms lies near or on the surface, which subsequently decrease the available interstitial octahedral sites for Li insertion in the bulk anatase. Since A6 has the largest specific surface area among all these powders, its larger amount of surface atoms thus reduced the octahedral sites for Li insertion, hence shortened the biphasic region on the discharge curve.

Based on the discharge curves, the process of Li insertion into nanocrystalline anatase electrodes can be divided into three stages. First, very small amount of Li ions (such as 0.07 Li per TiO_2 for A6) are associated with the initial monotonous potential decrease before the plateau (at ca. 1.78 V (Li^+/Li)). In fact, the capacity within this potential window is very large in the first discharge (0.22 Li per TiO_2 for A6, see Fig. 2), but decreases rapidly

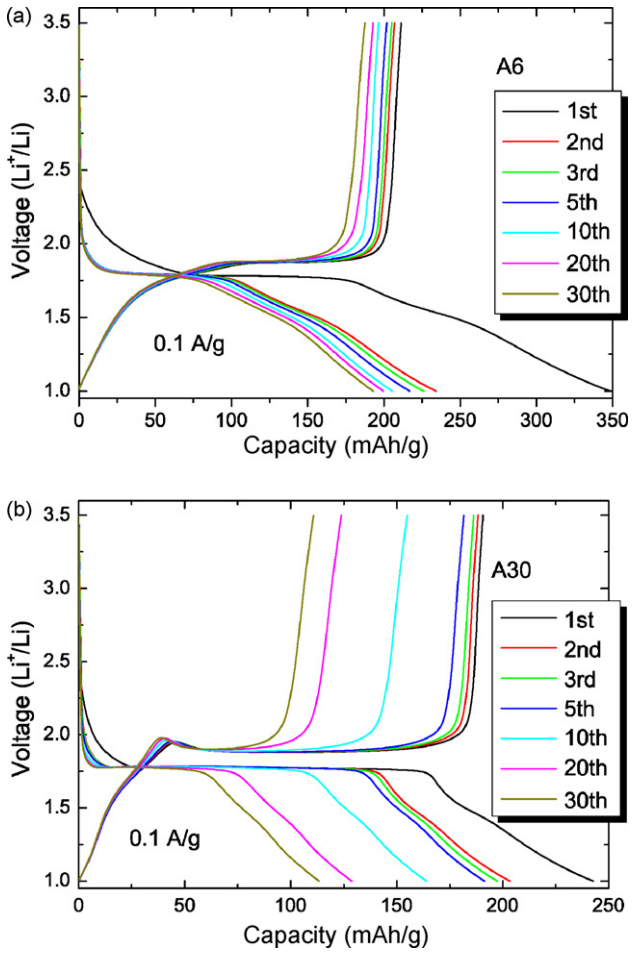

Fig. 2. The discharge–charge curves of (a) A6 and (b) A30 at various cycles that cycled at 0.1 A g^{-1}.

from the second cycle and is almost constant thereafter. Tarascon and coworkers [16] ascribed this region to the formation of solid solution domain of anatase TiO_2 and Li_xTiO_2. However, the capacity loss of this region in the first cycle suggests that the Li ions resided in this solid solution domain are mostly irreversible. A capacitive-like surface effect, i.e., EDLC, rather than the formation of solid solution domain, might be more plausible to explain the stable small capacities within this potential window from the second cycle since these small capacities are proportional to the specific surface areas of different electrodes and highly reversible.

The second stage is the Li insertion into the interstitial octahedral sites of the bulk anatase crystals, corresponding to the horizontal plateau at 1.78 V (Li^+/Li). This is a classical Faradaic process. The surface layer generates surface states at potentials negative from the flatband [5]; so in the third stage, after all the available interstitial octahedral sites inside the anatase crystals are filled, Li ions are further inserted into the surface layer under the external force of the electric field (the sloped region from 1.78 to 1.0 V (Li^+/Li)). Because decreasing the crystallite size can broaden the energy levels accessible in the materials, a wide voltage distribution at which the electrochemical reaction take place appears [16], which leads the discharge curve at the third stage to a long sloped region. From Fig. 1 it is clearly seen that the capacity of this sloped-region is increased with increasing the specific surface area of the anatase electrodes, confirming that the third stage of Li insertion is mainly a surface effect.

To investigate the capacity loss in anatase electrodes, Fig. 2a and b shows the voltage profiles of A6 and A30 at various cycles at the current density of 0.1 A g^{-1}. Let us study the charge curves only. For both electrodes, the sloped-region between 1.0 and 1.89 V (Li^+/Li), which is the reverse Li extraction process of the Li insertion between 1.78 and 1.0 V (Li^+/Li) during discharge, only changes slightly upon cycling. This indicates that the Li ions inserted into the surface layer are highly reversible except those being trapped in the initial insertion. The capacity decays are mainly caused by the shortening of the plateau in both electrodes. That means the Li ions inserted into the bulk of the anatase phase are gradually trapped and lose their reversibility with cycling. The length of the Li extraction plateau decreases much faster in A30 than that in A6, indicating that decreasing the particle size, i.e., reducing the Li diffusion length, has effectively improved the reversibility of the Li ions inserted into the bulk anatase, which in turn leads to a good capacity retention.

Besides the high capacity, nanocrystalline anatase electrodes also exhibit very promising high rate performances. Fig. 3 presents the current density dependence of the discharge capacities of different anatase electrodes. The data is extracted from the second discharge curves. Clearly, with decreasing the particle size, the high rate performance of nanocrystalline anatase electrode is significantly improved. The specific discharge capacity of A6 remains 209, 181 and 139 mAh g^{-1} at the current densities of 1 A g^{-1} (~6 C), 10 A g^{-1} (~60 C) and 40 A g^{-1} (~239 C), corresponding to 0.62, 0.54 and 0.41 mol Li in per mol of TiO_2, respectively. Even we restrict the cut-off voltage between 3.5 and 1.4 V (Li^+/Li), similar to that used in ref. [17], the specific discharge capacities of A6 are still 131 and 72 mAh g^{-1} at 10 and 40 A g^{-1}, respectively, being the best high rate performance ever reported in anatase TiO_2 electrodes.

Fig. 4a and b respectively shows the potential-capacity profiles of A6 and A30 at different current rates. Again, we study the

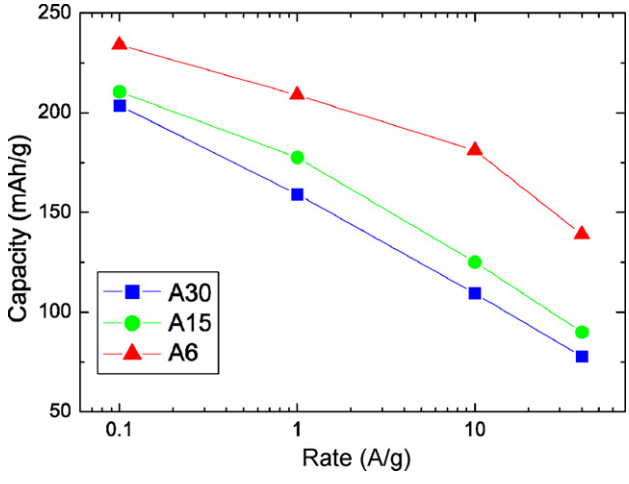

Fig. 3. The current density dependence of the discharge capacities of different anatase electrodes. The data is extracted from the second discharge process.

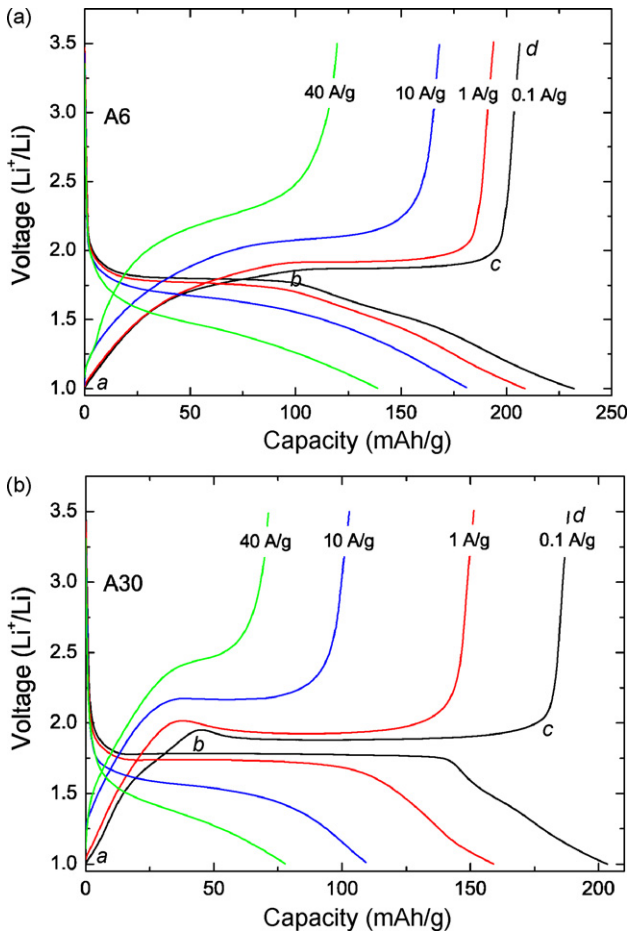

Fig. 4. The second discharge–charge curves of (a) A6 and (b) A30 that cycled at different current rates. Letter a to d label the transitions between different regions on the charge curves.

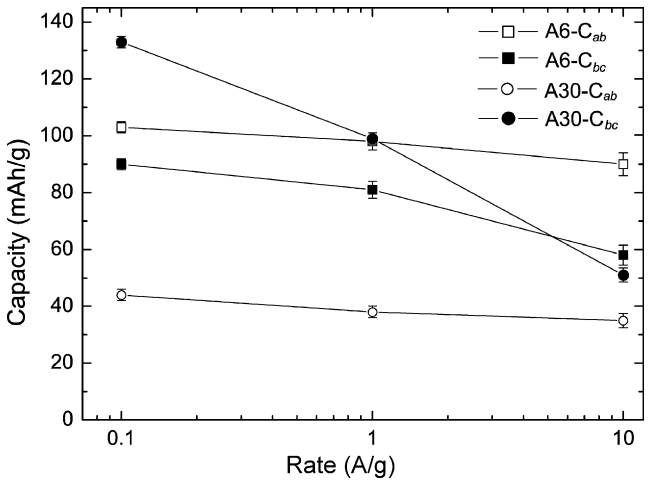

Fig. 5. The specific capacities of the sloped-region below the plateau (C_{ab}) and the plateau (C_{bc}) of A6 and A30 as a function of the current densities.

charge curves only. The charge capacity can be roughly divided into three parts, as labelled by a to d in Fig. 4: the sloped-region below the plateau (C_{ab}), the plateau (C_{bc}) and the sloped-region above the plateau (C_{cd}). Because the capacity above the plateau (C_{cd}) is rather small and almost does not change with the current rate, here we only consider C_{ab} and C_{bc}. Fig. 5 plots the C_{ab} and C_{bc} of A6 and A30 as a function of the current densities. Because no clear transitions between different parts on the charge curves can be found, the data of that cycled at 40 A g^{-1} is not included. As seen in Fig. 5, C_{ab} of A6 is much higher than that of A30, which is consistent with its larger specific surface area. Despite of that, C_{ab} of both electrodes only decrease slightly with increasing the current density, indicating that the capacity contributed by the surface Li storage is very stable and almost does not change with the current density. This means the surface Li storage only depends on the surface area while not on the diffusion time. On the contrary, the Li insertion/extraction in/from the bulk atatase is highly dependent on the diffusion time since it is a solid-state diffusion process. As seen in Fig. 5, C_{bc}s of both electrodes decrease upon increasing the current density. From this point of view, the surface Li storage has played a very important role on the high rate performance of the nanocrystalline anatase electrodes. From Fig. 5 we also note that C_{bc}s of A30 are higher than those of A6 at 0.1 and 1 A g^{-1}. This suggests that A30 has a higher ratio of interstitial octahedral sites than A6 for Li insertion/extraction inside the particles within the initial cycles at low current rates. However, with increasing the cycle number (see Fig. 2) or current density (see Fig. 4), C_{bc} of A30 drops much faster than that of A6. This indicates that the Li insertion/extraction only occurs in the outer layers of the particles at a high current rate due to the very short diffusion time. Because of the shorter Li diffusion length, most of the interstitial octahedral sites are still available for Li insertion in a very short time, so A6 shows a much slower decrease of C_{bc} with the current density. Our results demonstrate that besides increasing the specific surface area, reducing the Li diffusion length of the electrode materials is also important to facilitate the Li insertion/extraction and improve the high rate performance.

What we should point out here is the excellent high rate performance of the nanocrystalline anatase electrodes might be partially ascribed to the very low specific current density of the active material because of the very large surface area. For instance, the specific surface area of A6 is 258 m^2 g^{-1}. If the apparent area of the anatase electrode is 0.25 cm^2, for 1 mg active material, the effective current density of the active material is only about 10^{-4} of the applied current density of an electrode (here we even did not consider the effect of AB in the reduction of the current density) [13]. Such a low specific current density can effectively stabilize the electrode and preserve a high capacity at the high rate discharge–charge current density.

As discussed above, C_{ab} is very stable upon cycling in all the electrodes. Meanwhile, decreasing the Li diffusion length may greatly stabilize C_{bc}. These two features of the nanocrystalline anatase electrodes are expected to yield a good cyclability. Fig. 6 shows the cycle performance of different anatase electrodes at 10 A g^{-1}. After 100 cycles, the discharge capacity of A6 is still of 125 mAh g^{-1}, corresponding to 0.37 Li in per TiO_2. This value is 80 mAh g^{-1} in A15 and 71 mAh g^{-1} in A30, respectively. The capacity retention of A6 is higher than 95% from the third cycle, and higher than 99% after the tenth cycle. The stable cycle performance of A6 even at high discharge–charge current rate

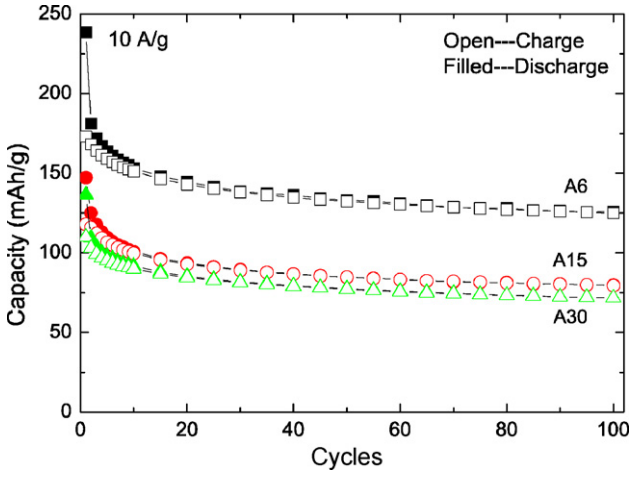

Fig. 6. Cycle performance of the nanocrystalline anatase electrodes with different particle sizes cycled at 10 A g^{-1}.

is well consistent with its high specific surface area and short Li diffusion length. The excellent high rate capacity and cyclability render nanocrystalline anatase a promising anode material for Li-ion battery for high power and high energy density use.

4. Conclusion

A systematic study of the particle size effect of nanocrystalline anatase TiO_2 electrodes on the lithium storage capability and high rate performance was conducted. The results indicated that using ultrafine anatase powders like 6 nm as the electrode materials can effectively improve the surface Li storage and facilitate the Li insertion/extraction in/from the interstitial octahedral sites in the bulk anatase phase. The capacity contributed by the surface Li storage is very stable upon cycling and increasing the discharge–charge current densities, so it plays a very important role on the high rate performance and cyclability. Our results are well consistent with the concept that the rate performance and cyclability of Li-ion batteries can be significantly improved by reducing the Li diffusion length and increasing the specific surface area of the active materials by using nanostructured electrodes.

Acknowledgements

This work is financially supported by the New Energy and Industrial Technology Development Organization (NEDO). C.H. Jiang thanks Drs. S. Shimano, E. Hosono, T. Watanabe, and Mr. M. Ichihara for their helps on the experiments.

References

[1] T. Ohzuku, Z. Takehara, S. Yoshizawa, Electrochim. Acta 24 (1979) 219.
[2] F. Bonino, L. Busani, M. Lazzari, M. Manstretta, B. Rivolta, J. Power Sources 6 (1981) 261.
[3] B. Zachau-Christiansen, K. West, T. Jacobsen, S. Atlung, Solid State Ionics 28–30 (1988) 1176.
[4] W.J. Macklin, R.J. Neat, Solid State Ionics 53–56 (1992) 694.
[5] R. van de Krol, A. Goossens, J. Schoonman, J. Phys. Chem. B 103 (1999) 7151.
[6] T. Ohzuku, T. Kodama, T. Hitai, J. Power Sources 14 (1985) 153.
[7] M. Wagemaker, R. van de Krol, A.P.M. Kentgens, Ad.A. van Well, F.M. Mulder, J. Am. Chem. Soc. 123 (2001) 11454.
[8] M. Wagemaker, G.J. Kearley, Ad.A. van Well, H. Mulka, F.M. Mulder, J. Am. Chem. Soc. 125 (2003) 840.
[9] L. Kavan, M. Gratzel, S.E. Gilbert, C. Klemenz, H.J. Scheel, J. Am. Chem. Soc. 118 (1996) 6716.
[10] A. Stashans, S. Lunell, R. Bergstrom, Phys. Rev. B 53 (1996) 159.
[11] R.J. Cava, D.W. Murphy, S. Zahurak, A. Santoro, R.S. Roth, J. Solid State Chem. 53 (1984) 64.
[12] H. Lindstrom, S. Sodergrem, A. Solbrand, H. Rensmo, J. Hjelm, A. Hagfeldt, S.E. Lindquist, J. Phys. Chem. B 101 (1997) 7717.
[13] H. Zhou, D. Li, M. Hibino, I. Honma, Angew. Chem. Int. Ed. 44 (2005) 792.
[14] L. Kavan, M. Gratzel, J. Rathousky, A. Zukal, J. Electrochem. Soc. 143 (1996) 394.
[15] L. Kavan, M. Kalbac, M. Zukalova, I. Exnar, V. Lorenzen, R. Nesper, M. Gratzel, Chem. Mater. 16 (2004) 477.
[16] G. Sudant, E. Baudrin, D. Larcher, J.M. Tarascon, J. Mater. Chem. 15 (2005) 1263.
[17] I. Moriguchi, R. Hidaka, H. Yamada, T. Kudo, H. Murakami, N. Nakashima, Adv. Mater. 18 (2006) 69.
[18] V. Subramanian, A. Karki, K.I. Gnanasekar, F.P. Eddy, B. Rambabu, J. Power Sources 159 (2006) 186.